Cement and Concrete Research 39 (2009) 1239–1249

Contents lists available at ScienceDirect

Cement and Concrete Research

journal homepage: http://ees.elsevier.com/CEMCON/default.asp

Revealing the temperature history in concrete after fire exposure by microscopic analysis

E. Annerel *, L. Taerwe

Ghent University, Department of Structural Engineering. Faculty of Engineering, Magnel Laboratory for Concrete Research, Technologiepark Zwijnaarde 904, B-9052, Ghent, Belgium

ARTICLE INFO

Article history:
Received 10 February 2009
Accepted 25 August 2009

Keywords:
Temperature
SEM
EDX
X-Ray Diffraction
Petrography

ABSTRACT

Concrete structures behave in most cases very well during a fire, after which it is often possible to repair or strengthen the structure to a certain level. This could result in important economic benefits, as costs for demolition and rebuilding can be avoided and the building can be reused faster. In this paper three methods for determining the maximum temperature to which a concrete structure was submitted during a fire are studied. Knowledge of the temperature distribution is necessary to assess the overall damage of a concrete structure. First, the physico-chemical transformations of heated concrete are investigated with scanning electron microscopy (SEM). Secondly, the features visible under the polarising and fluorescent microscope (PFM) are discussed. And third, the influence of heat on the colour of the aggregates is analysed.

1. Introduction

Although the probability of occurrence of a fire may be small, its impact on a structure is high. Several cases in the recent past show the effect of such an accident on civil structures, for instance tunnels (Mont Blanc 1999, St. Gothard Pass 2001, and Frejus 2005) and high-rise buildings (Ostankino Television Tower 2000, Pirelli Skyscraper 2002, and Windsor Tower 2005). This problem not only affects our environment and safety, but also has serious socio-economic consequences due to the disruption of the traffic for many weeks or months and of the occupancy of a building. However, concrete structures in most cases behave very well during a fire and although they suffer from a certain degree of strength loss, it could be interesting to repair these structures. Repair shows some economic benefits, since costs of demolition and rebuilding can be avoided, and the building can be reused in a shorter time period [1]. Repair of damaged concrete is traditionally done with shotcrete. A real fire experiment in the 1970's studied how a precast concrete building survives a fire, after which elements were repaired and tested for residual strength. A typical large pretensioned roof beam had a residual strength almost equal to the original strength, thus showing the possibilities of concrete repair [2].

The state of a concrete structure should be assessed to quantify the degree of damage, since this will determine the repair costs. Thus, an overall damage assessment is necessary to estimate the costs of repair or demolition. This paper describes the fundamental knowledge to do such an assessment appropriately, based on destructive core drilling.

The effect of fire on the strength of traditional concrete has been studied for many years and typical strength loss models are described in building codes [3]. However, the residual strength is influenced by the moisture conditions during the storage period after cooling and could result in an additional drop of 20–30% [4]. For assessment of the strength of a concrete element after fire, it is important to consider the heating profile of the member. Since the element is mostly heated from one side, a temperature gradient will occur in the concrete during the fire. Direct compressive tests on cores drilled from an element are not adequate, since they do not give the average value over the cross section as the failure is in the heated region of the core. The resulted strength is thus not representative for the whole element. Another philosophy — an indirect method — is thus necessary. Since the strength loss can be related to the temperature, changes due to the temperature history should be examined. When concrete is heated, chemical and mineralogical changes will occur, which must be determined and quantified. This chemical behaviour of concrete during a fire can be observed by thermal analysis (DTA/TGA), as was studied by Liu [5] and other authors. Certain phases of the concrete will convert into new ones which may alter the colour of the concrete, the (original) mineralogical composition of the cement paste and its porosity. Microscopy has proven to be a useful tool to track most of the changes [6]. This paper describes and illustrates the main features which become visible by microscopic analysis.

On a macroscopic level, other features are discernible, such as the change in colour and porosity. The colour changes from red at temperatures between 300 °C to 600 °C to whitish grey around 600 °C to 900 °C and buff at 900 °C to 1000 °C [7]. The reddish colour is assumed to be caused by the oxidation of the iron hydroxides in the aggregates and the cement paste. Since 300 °C is commonly the onset of a significant concrete strength loss, traditional repair is based on

* Corresponding author. Tel.: +32 (0) 9 264 55 19; Fax: +32 (0) 9 264 58 45.
E-mail address: emmanuel.annerel@ugent.be (E. Annerel).

0008-8846/$ – see front matter © 2009 Elsevier Ltd. All rights reserved.
doi:10.1016/j.cemconres.2009.08.017

cutting the damaged concrete to the depth of red colour [1]. The whitish grey discoloration of the concrete should be attributed to the disintegration of the calcareous constituents of the aggregate and cement paste. This paper studies the colour path of siliceous and calcareous aggregates when heating up to 1150 °C. The mineralogy and chemical composition of the aggregates are determined by X-ray diffraction (XRD) and Energy Dispersive X-ray spectroscopy (EDX).

The phase changes due to heating of the cement paste are influenced by the way moisture is captured inside the concrete element. The transformations of the aggregates are not influenced by this. A distinction should be made between unsealed conditions that allow the cement paste to dry and sealed conditions where no moisture exchange with the environment is possible. This latter case may occur in massive concrete structures, at a sufficient depth from the surface. The observed phase transformations of the cement matrix in this paper are only valid for unsealed conditions. The outlined techniques related to the degradation of the cement paste are thus available for diagnosis close to the surface, at a depth to which important damage due to fire could occur. Further, the transport of water is of influence for relatively low temperatures (<120 °C), where it causes a strength loss if heated for short periods and a strength development if heated for at least 3 days. For high temperatures (>250 °C), the free water has already been vaporized and is, therefore, of no further influence. Notice that this happens at temperatures beneath the actual degradation of the portlandite (peak at 450 °C) and the development of significant cracks around the perimeter of the aggregates (300 °C). Moreover, the drying process retards the temperature increase inside the concrete. For sealed conditions, the phase changes are determined by the CaO/SiO_2 ratio, as is discussed in [9].

2. Scanning electron microscopy

One hundred and fifty litres of traditionally vibrated concrete composed of siliceous sand, siliceous gravel and Portland cement is cast in cubes of 150 mm side length. The concrete mix design is given in Table 1. The cubes are cured for 4 weeks in an air-conditioned room at RH >90% and a temperature of 20±1 °C, after which they are stored at 60% RH and 20±1 °C for drying. From the cubes, rectangular samples with dimensions of 120×120×25 mm are cut and heated at an age of 10 months after casting. Different target temperatures (20 °C, 175 °C, 250 °C, 350 °C, 450 °C and 550 °C) are held constant until a uniform temperature distribution inside the concrete is reached. The heating rate is initially equal to 40 °C/min and is slowed down to 20 °C/min at 530 °C. The samples are left in the oven after heating, thus allowing the samples to cool slowly. After cooling, the samples are kept in atmospheric conditions until further testing.

From these samples, a fresh fractured surface is obtained, which is studied with a Philips-XL30-ESEM at high magnification (×2000). This type of microscope allows one to see the microstructure on the level of the capillary pores. Fig. 1 depicts the interfacial transition zone (about 45 µm) of a traditional concrete at ambient temperature and after heating to 350 °C and 550 °C. At 20 °C, the cement matrix is intact and is constituted of ettringite, CH and CSH. Around 350 °C, a more coarsened cement matrix and the disappearance of ettringite are found. The ettringite already starts to break down at temperatures around 70 °C [6]. At 550 °C, the CH has also been disintegrated (>450 °C), resulting in a cement matrix with a very porous structure. However, at 550 °C some CH remnants could remain, since TGA/DTA analysis show that the dissociation of CH is spread between 400 °C and 600 °C [9]. This is especially the case in the interfacial zone, because there the CH is more concentrated due to the higher porosity compared to the bulk of the cement stone. When temperature increases, the depletion of the hydration products makes room for

Table 1
Concrete mix design.

	OPC concrete
Siliceous sand 0/4 [kg/m³]	640
Siliceous gravel 2/8 mm [kg/m³]	525
Siliceous gravel 8/16 mm [kg/m³]	700
Portland cement I 52.5 [kg/m³]	350
Water [kg/m³]	165
W/C [–]	0.47
Slump [mm]	40
Air content [%]	2
Density [kg/m³]	2400
Flow	1.4
$f_{ccub150}$ 28 days [N/mm²]	52.8
Density 28 days [kg/m³]	2374

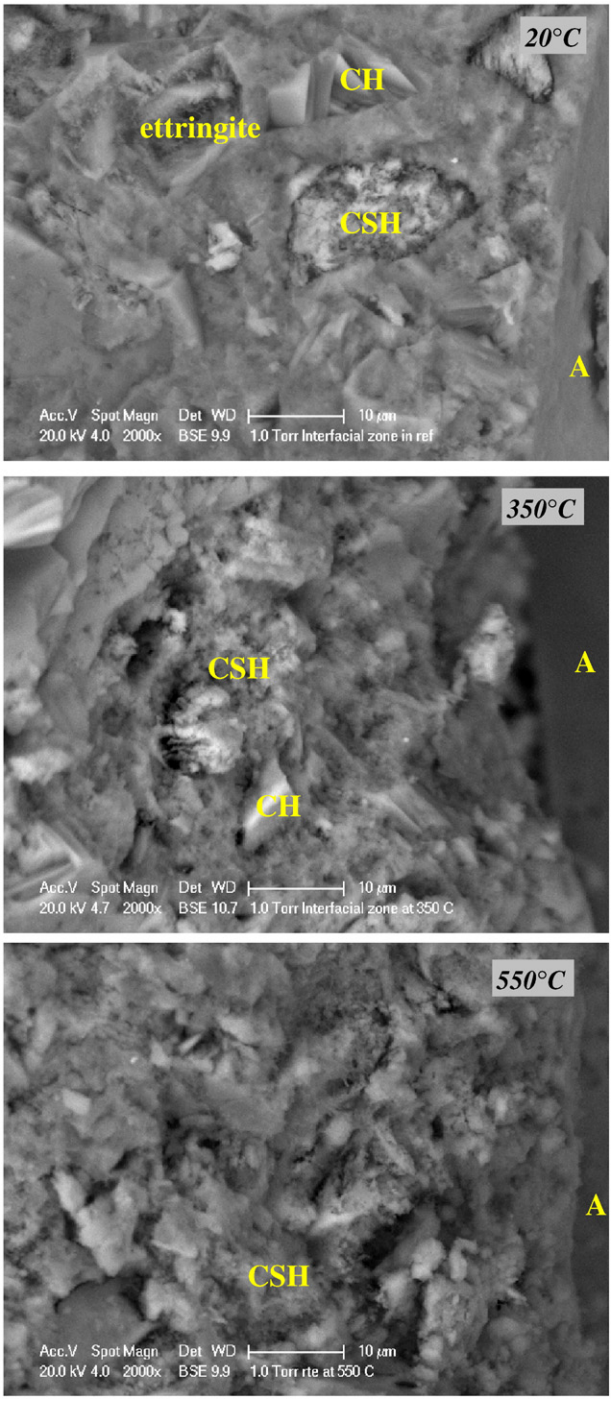

Fig. 1. OPC cement matrix in the interfacial transition zone at 20 °C, 350 °C and 550 °C.

additional pore space, as is discernible on the images by the increase of black spots.

Liu [5] studied the depletion of the phases of heated (up to 500 °C) cement pastes (traditional, self-compacting and high strength) by a threshold method. This method is described in [8] and consists of deriving from the SEM images a histogram of the greyscale intensity. For a polished cement paste sample (dried and impregnated with epoxy resin) the anhydrous phases of the unhydrated cement appear bright, the calcium hydroxide light grey, the C–S–H dark grey and the pores black. Segmenting the SEM images on the different greyscale ranges permits the quantification of these phases. At a 500× magnification, an overall increase of the capillary pore phase and a decrease of the hydrated products in the temperature region from 130 °C to 500 °C is found. Furthermore, the amount of unhydrated cement and the amount of limestone filler (in the self-compacting cement paste) are constant, because the decomposition of the $CaCO_3$ in the filler starts only at about 700 °C. Once calibrated with the actual concrete in the investigated structure, this technique could help to assess the temperature history in heated concrete.

Besides the changes in porosity, heated concrete suffers from cracking. Two types of cracks can be distinguished: cracks around the perimeter of the coarse aggregates (interfacial cracks) and cracks in the cement matrix (cement matrix cracks). Fig. 2 illustrates the interfacial transition zone at a 250× magnification with SEM. The crack development around the aggregates and in the cement matrix is visible. At 20 °C, the cement matrix and the bonding is intact, whereas the aggregate in the right corner of the image shows an initial crack. At 350 °C, other cracks appear, which only get more severe at 550 °C. An adequate bond between the cement stone and the aggregates is of great importance for the behaviour of concrete during fire. The aggregate–cement transition zone is normally weaker (more porous) than the bulk of the cement stone, as can be noticed from PFM (Fig. 5, left). At higher temperatures, this bond fails mostly due to thermal incompatibilities and dissociation of the cement matrix (loss of CH), resulting in cracking around the aggregates perimeter and consequently leading to a significant strength reduction. Heating concrete also causes cracks in the cement matrix, which start around the fine aggregates and are probably also due to the difference in thermal expansion. Further, the samples are exposed to moisture from the air before studying with the microscope. This post-cooling exposure results in further strength loss of the concrete due to the formation of new portlandite that is accompanied with a 44% volume increase [4,9]. The cracks in the studied specimens are thus the combined effect of thermal incompatibility, and degradation of the cement matrix during and after heating.

The prediction of the cracks in concrete exposed to fire is, nonetheless, more complicated. The samples studied in this paper have small dimensions and are unloaded during the heating process. However, in reality, concrete is used as a structural material. When loaded concrete is heated, less strength reduction is observed, appearing at smaller strain levels. Load Induced Thermal Strain (LITS) is the principle behind this phenomenon [9] and results probably in less cracking. However, this should be further investigated, because the weight increase of cubes during 28 days of storage in air (20 ± 1 °C, 60% R.H.) or under water, heated to 350 °C and 550 °C under a load of 0% and 20% of the initial strength before heating showed only small differences or higher increases for 20% load. For a high performance concrete composed of siliceous aggregates and Portland cement, storage in air after heating for 12 h at 350 °C resulted in an increase of the moisture absorption of 0.32% for 0% load and 0.36% for 20% load. For storage under water, an increase is found of 5.45% for 0% load and 4.7% for 20% load. At 550 °C, an increase of 0.87% for 0% load and 0.5% for 20% load is observed for storage in air, while for storage in water, this is respectively 4.07% and 11.6%. Remark that LITS only takes place during first time heating and for concrete under compression [9]. LITS is thus mostly important for

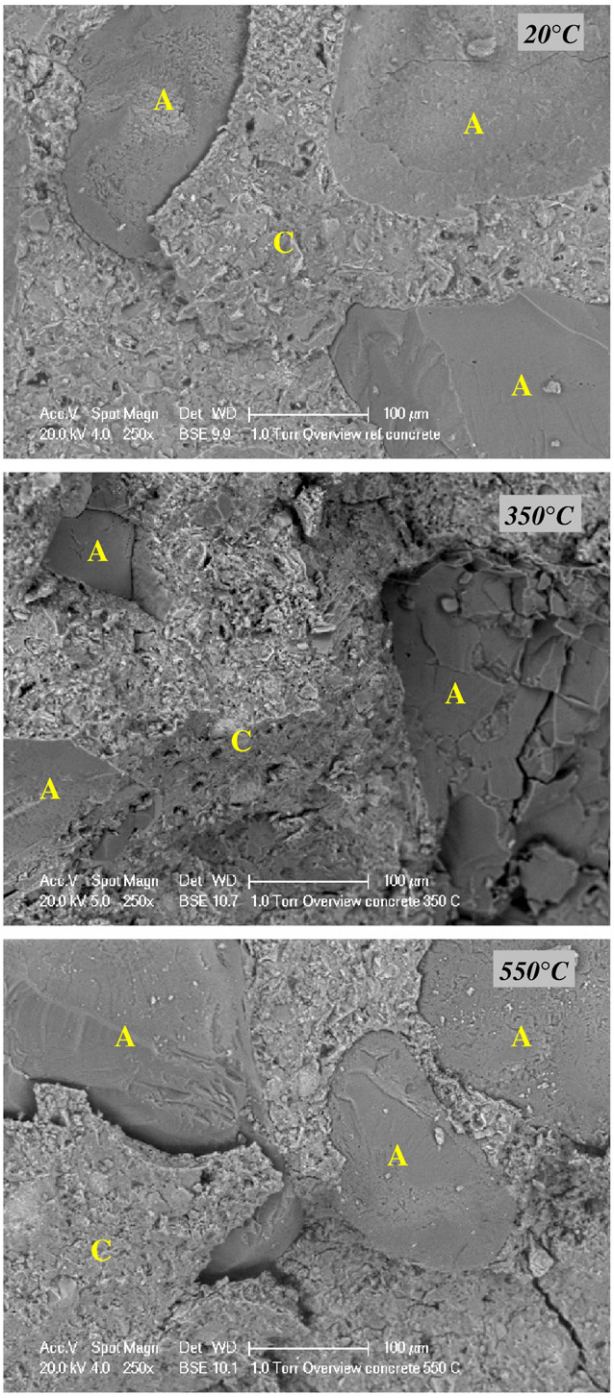

Fig. 2. Overview of OPC concrete at 20 °C, 350 °C and 550 °C. (A: aggregate, C: cement matrix)

columns. Other elements, such as beams and slabs, have generally compressive stresses only at the top layers. In these cases, the effect of LITS is less, since these compressive stresses occur in a gradient and are located further away from the fire. LITS does thus not occur at the bottom layers, which are closest to the fire and are of most importance for an expertise to trace the temperature history inside the element. In these cases, the study of the crack behaviour of unloaded samples, as provided in this paper, is more relevant. Another phenomenon related to large elements is spalling which is also highly depended on the moisture content. Cracks may occur due to the combined effect of the increase of pore pressures and external loading [9]. Further, loaded structural elements may endure cracking due to mechanical actions,

such as bending moments and shear. Both actions are influenced during fire when the free thermal expansion of the element is restrained, leading to curvatures to the fire and possibly shear failure in columns [10]. Also, internal cracking is possible due to the difference in displacement between the inner cold concrete and the heated outside layers, resulting in tensile stresses which are not located in the neighbourhood of the reinforcement [10]. These mechanical actions, however, lead to other crack patterns than observed on the studied samples.

3. Polarising and fluorescent microscopy

With the polarising and fluorescent microscope, it is possible to study thin sections from drilled cores with 3 types of light setting: plain polarised transmitted light (PPTL), UV fluorescent light (UVFL) and cross polarised light (CPL). Table 2 covers the diagnostic features which are noticeable with the optical microscope [5,9].

Under PPTL, the air bubbles and cracks are clearly visible as yellow spots due to the intrusion of the epoxy. The air bubbles at 20 °C show some ettringite in the pores, noticeable as needles (Fig. 3). At about 70 °C, the ettringite starts to break down and will disappear completely at higher temperatures. The development of the cracks around the fine and coarse aggregates can be studied with this light setting (Fig. 4). At relatively low temperatures (175 °C), the interfacial cracks are not entirely developed around the perimeter of the aggregate. However, at high temperatures (550 °C) the debonding can be complete, leading to the breaking loose of some aggregates. These interfacial cracks can get connected through the cement matrix when situated near the surface, resulting in scaling of the concrete surface. This scaling may be influenced by the moisture content and the distance to the concrete surface. In the concrete mass, this scaling is hindered by the surrounding material. This phenomenon was already noticed at 175 °C (Fig. 4, left).

Under UVFL, the air bubbles and the cracks are coloured pale green and contrast with the background. The intensity of green colour is linked with the porosity, whereas aggregates colour black. At ambient temperatures, the green colour in the bulk of the cement matrix is darker than in the transition zone (Fig. 5, left). The interfacial transition zone must therefore be more porous. At higher temperatures, the free water evaporates and cracks appear, turning the whole cement matrix a light green colour (Fig. 5, right). The PFM magnifies to about 1 µm, which allows one to study the air voids and part of the capillary pores. The intensity of the green colour can be plotted in a histogram, from which the fluorescence index can be derived. This technique is widely used for the determination of the water–cement ratio of a concrete sample at ambient temperatures by means of some reference samples and a calibration curve [11,12]. Fig. 6 shows the fluorescence intensity determined at different temperatures, relative to the fluorescence at 20 °C. This process is executed for ×100 and ×400 magnification. Above 100 °C, this intensity increases due to the loss of free water, from where it has a small drop and remains more or less constant. Furthermore, this trend does not change significantly when altering the magnification or even considering the cracks into the fluorescence index. UVFL can thus only be used to determine whether the temperature of 100–130 °C has been exceeded.

Table 2
Diagnostic tracers for petrography [6,9].

Temperature [°C]	Macro- or microscopically diagnostic features	Figure
70–80	Dissociation of ettringite, leading to the disappearance of small spines which are developed in air bubbles during hydration. Visible under PPTL	5
>105	The loss of physically bound water in aggregate and cement paste causes an increase in the micro-cracking and capillary porosity of the cement paste.	7
120–163	Dissociation of gypsum, causing its depletion in the cement paste	
>300	Marked increase in porosity and micro-cracking	6
300–350	Oxidation of FeOOH to α-Fe_2O_3: change in colour to pink or reddish brown and disconnection of the sand particles	9, 10
400–600	Dissociation of portlandite, causing its depletion in the cement paste	11

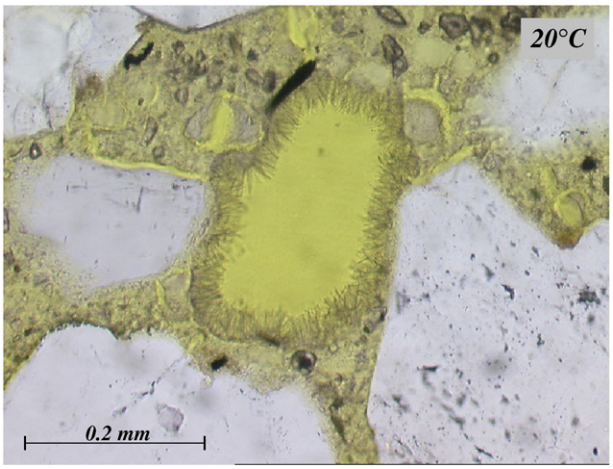

Fig. 3. PPTL: presence of ettringite in air bubbles at 20 °C.

Siliceous aggregates can be constituted of sand particles which are glued together by a binding agent. If this binding agent is calcite $CaCO_3$ or clay with FeOOH, there is a difference in material between the binding agent and the sand particles. When such aggregates are heated to 300–350 °C, cracks will occur around the sand particles due to differences in thermal expansion and the process of expansion and shrinkage caused by the loss of water in the clay. Under UVFL, this disconnection of the different sand particles is visible (Fig. 7). Meanwhile, the FeOOH oxidizes, resulting in a typical reddish discoloration. This colour change of the binding agent marks the boundaries of the different sand particles as discernible under PPTL (Fig. 8). On the other hand, if the binding agent is silica, the material of the binding agent and the sand particles is the same, resulting in no internal stresses and no crack development in the aggregate. Since there is also no iron, no change of colour will appear. The reddish brown discoloration can be seen as a measure of the amount and location of iron in the aggregate. Due to the stresses caused by the breaking of the aggregates, a crack started in the aggregate can continue through the cement matrix (Fig. 8, left).

Under CPL, portlandite ($Ca(OH)_2$) is visible as white spots in the cement matrix. During the hydration process, the portlandite crystallizes in the voids of the cement matrix which is most porous at the interfacial transition zone. When concrete is heated beyond 400 °C, the portlandite starts to dissociate. However, remnants are possible, especially in the interfacial transition zone, because of the higher amount of portlandite (Fig. 9, right). In the end, all the portlandite will diminish if the heating lasts long enough.

In relation to TGA/DTA analysis [5,9], microscopic analysis yields some advantages since one single thin section provides information over the thickness of the exposed element. Under the microscope, the transformations are visible, starting at the surface and then further into the concrete thickness. This way, different isotherms can be noticed, namely >70 °C (dissociation of ettringite), 100–130 °C (increase of fluorescent index), 300–350 °C (red colouration of siliceous aggregates) and 400–600 °C (depletion of portlandite). TGA/DTA results in similar temperature regions. However, to trace the isotherms at different depths, one analysis is not enough and should be repeated at each depth. The advantage of this technique is the possibility to distinct the original portlandite from newly formed

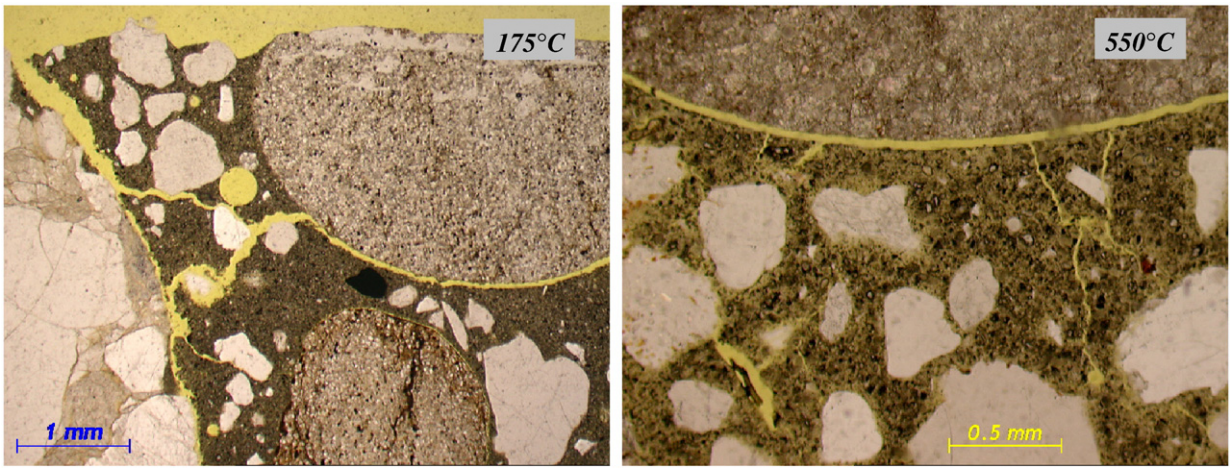

Fig. 4. PPTL: development of cracks around the aggregates and in the cement matrix.

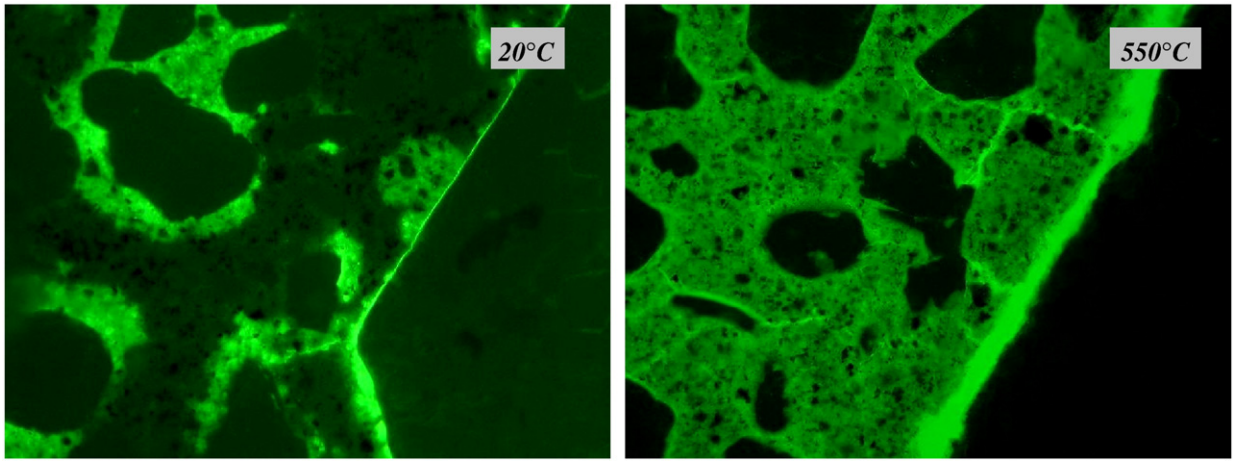

Fig. 5. UVFL: development of cracks and increase of fluorescence intensity (magnification ×100).

portlandite during post-cooling storage after heating, since according to [13] the onset temperature of decomposition drops from 450 °C to 386 °C. Regarding this, it could be interesting to use petrography to trace the isotherms and to use TGA/DTA as a confirmation of the status of the portlandite.

4. Colour change of aggregates

Not only the cement paste, but also the aggregates suffer from physico-chemical degradations. The choice of aggregate is important, since various types of aggregate will be thermally stable up to different temperatures. Siliceous sands and aggregates, such as gravel, sandstones and quartzite rocks, are mainly constituted of quartz (SiO_2), but may have additional minerals. Sandstones, for instance, are formed from separate sand particles that are glued together with a binding agent which may contain iron oxides. Siliceous limestone is composed of quartz and an important amount of calcite ($CaCO_3$). The behaviour of the aggregates is therefore determined by the phase changes of its constituents, which occur at the following temperatures:

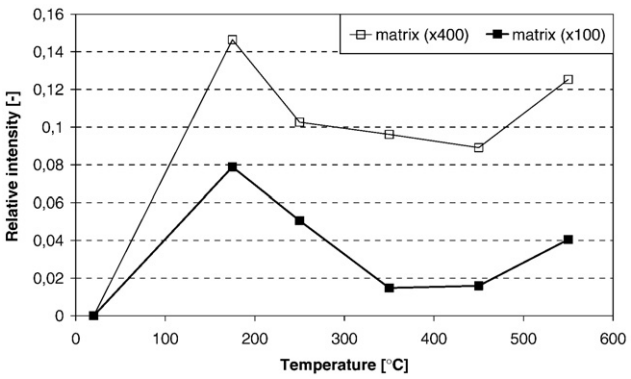

Fig. 6. Fluorescence intensity at different temperatures.

- 300–350 °C: oxidation of the iron hydroxides in sandstones, such as goethite α-FeOOH and lepidocrocite γ-FeOOH, to hematite α-Fe_2O_3, resulting in a pinkish to reddish brown coloration. Fig. 10 shows an ESEM recording of the iron in a sandstone heated to 350 °C, recognisable by the light grey colour.
- 573 °C: SiO_2 experiences an endothermic crystalline α–β phase transformation, which is accompanied by an instantaneous increase in volume of about 5.7%. This transition is reversible, but the radial cracks around the quartz grains caused by the expansion can be traced after cooling.
- 700 °C: dissociation of calcium carbonates, resulting in a considerable contraction due to the release of CO_2. The reaction reaches a peak at about 800 °C and is completed by 900 °C. Combined with atmospheric moisture during cooling, deterioration will most likely occur due to the formation of CH (44% increase in volume).
- >1050 °C: second phase change of SiO_2: formation of α-cristobalite, resulting in an expansion.

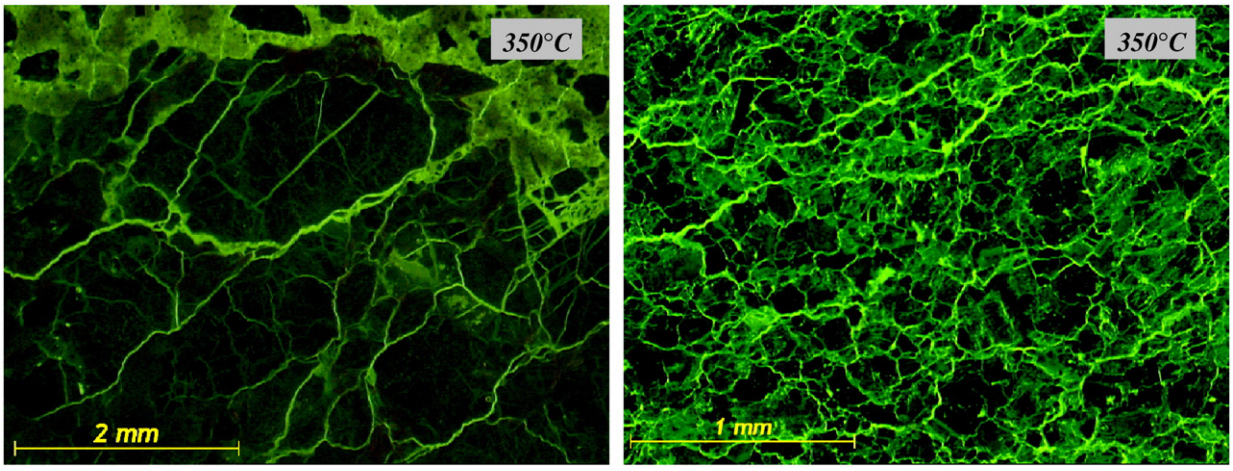

Fig. 7. UVFL: disconnection of the different sand particles in siliceous aggregates at 350 °C.

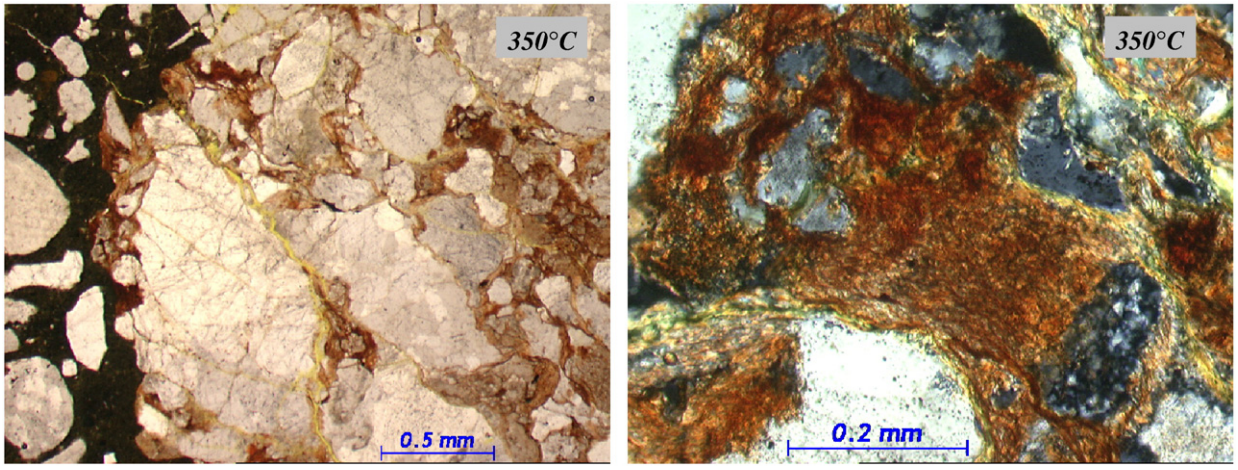

Fig. 8. PPTL: brown reddish coloration of the siliceous aggregates at 350 °C.

Siliceous gravel contains various colours. When these colourful aggregates are heated, the colour of some of them visually change. This is mostly to a reddish tint, which is determined by the oxidation of the iron at 300 °C. However, the colour remains altered when heated to higher temperatures. The colour change could be used to determine the temperature history of the heated concrete. Since most aggregates turn to a more reddish tint, the colours should be quantified in a scientific way. The composition of the aggregates must also be studied to distinguish two aggregates with the same amount of red, but heated to different temperatures.

From a batch of siliceous gravel, aggregates are selected on the basis of their colour after wetting: white, white–yellow, yellow–

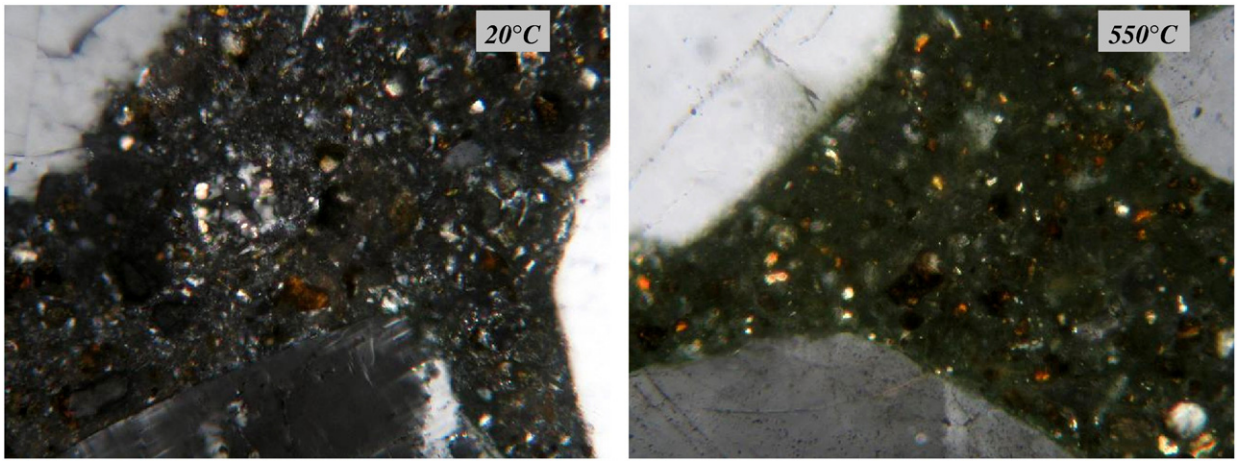

Fig. 9. CPL: difference in amount of portlandite at 20 °C and 550 °C (magnification ×400).

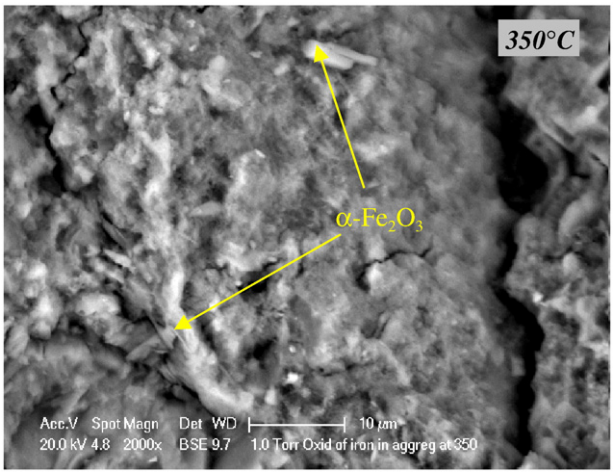

Fig. 10. Iron structure in a siliceous aggregate at 350 °C.

brown, brown–iron, brown, red, blue and green. These colours are most represented in the batch. The aggregate brown–iron is a sandstone, since different particles of sand as well as small spots of iron could be noticed with the naked eye. After crushing the aggregates into powder, the composition of the unheated aggregates is determined with XRD analysis and EDX. It should be noticed that the colour of the aggregates 'blue' and 'white–yellow' change, due to the grinding process, into respectively a brown–grey and grey tint.

The XRD patterns of all the aggregates show an adequate amount of quartz (SiO_2) which could be expected from siliceous gravel. Fig. 11 depicts the XRD pattern of some of the aggregates. Only the large peaks are visible on the graph, which corresponds with the XRD pattern of SiO_2. Table 3 presents the detected minerals for all the aggregates, from which 4 groups with the same constitution can be found. Group 1 consists of aggregates constituted of only quartz, namely the aggregates 'white' and 'white–yellow'. Group 2 covers the aggregates 'yellow–brown' and 'brown–iron', which are composed of quartz and sanidine ($KAlSi_3O_8$). Group 3 contains the aggregates 'brown', 'red' and 'blue', which are siliceous limestones, since they are built from both quartz and calcite. Group 4 is the aggregate 'green' and is made from quartz and corundophilite. Quartz, sanidine and corundophilite ($(Mg,Fe,Al)_6(Al,Si)_4O_{10}(OH)_8$) are minerals belonging to the silicate class, while calcite ($CaCO_3$) belongs to the carbonates class. Fig. 12 shows the XRD patterns for each group separately. These diffraction patterns are plotted with focus on the smaller peaks and show the differences per group, such as additional peaks and variety in peak height. Notice that in Fig. 11 one aggregate of each group is represented. Tests are performed on unheated samples and after heating to 550 °C. No differences in XRD pattern exist, except for the green aggregate, which is visible on the last graph.

The amount of iron in the aggregates is not detected with XRD, probably due to too small amounts. However, since the oxidation of the iron has an important effect on the discoloration, it is necessary to detect the iron. The use of EDX solves this problem. The powder of the aggregates is adhered to a carbon strip, scanned under a SEM in low vacuum mode at 2000× magnification (Fig. 13) and analysed with EDX. This mounting procedure combined with the grinding of the aggregates should produce a distribution of the atoms that is homogeneous. Fig. 13 shows an example of the peaks detected with EDX, which is the concentration of the atoms found on the carbon strip. Table 4 presents the atoms of the investigated aggregates in percentage as an average of 2 measurements. The values are derived from the EDX graph, with exclusion of the peaks of carbon (C) and oxygen (O). The C and O peaks are not counted, because their number of atoms is influenced by the sample preparation (carbon strip) and the oxygen from the air in the SEM chamber. The EDX is a fast method to determine the atomic composition of the aggregates. The outcome of an EDX analysis is semi-quantitative and the values provide the mutual ratio of the selected atoms. It is therefore not an absolute quantitative measurement of the composition, since not all types of

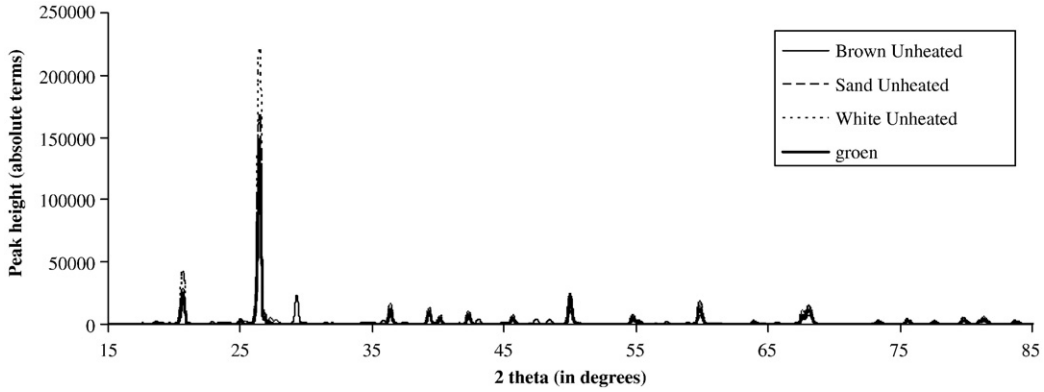

Fig. 11. XRD pattern of SiO_2.

Table 3
Results XRD analysis.

	Group 1		Group 2		Group 3			Group 4
	White[a]	White–yellow[a]	Yellow–brown	Brown–iron	Brown[a]	Red	Blue	Green
Quartz alpha SiO_2	x	x	x	x	x	x	x	x
Sanidine, disordered $KAlSi_3O_8$	–	–	x	x	–	–	–	–
Calcite $CaCO_3$	–	–	–	–	x	x	x	–
Corundophilite[b]	–	–	–	–	–	–	–	x

[a] Unknown peak at $\theta = 24°$.
[b] $(Mg,Fe,Al)_6(Al,Si)_4O_{10}(OH)_8$.

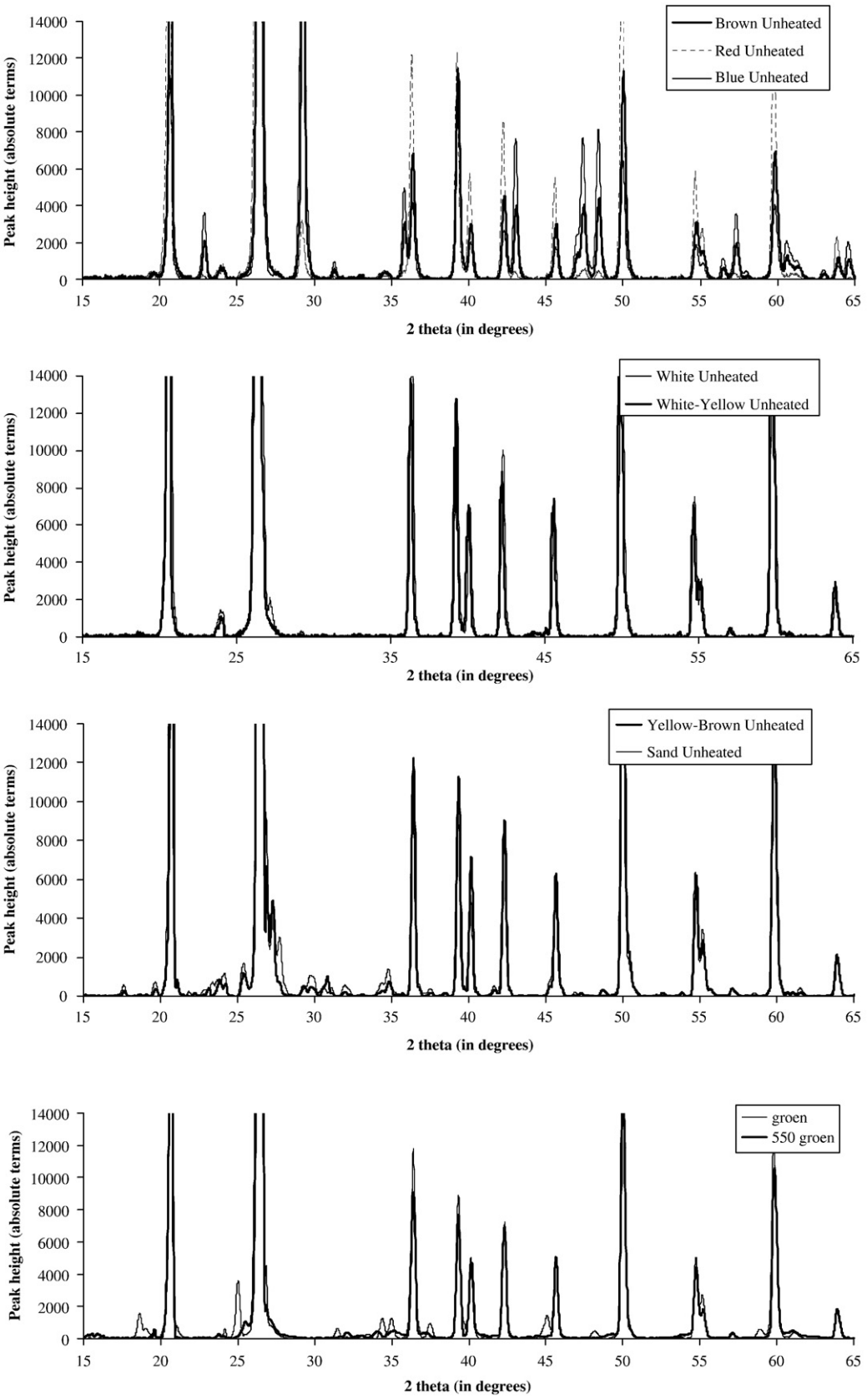

Fig. 12. XRD pattern of the aggregate groups.

atoms are considered. The results allow a division of the aggregates into certain groups and are useful to identify aggregates, even when the colour has changed after heating. The same groups as mentioned above can be found. Group 1 is characterised by silicon Si with a mutual ratio of around 97 %. The aggregates from group 2 have the same ions (Al, Si, K and Fe), in a comparable proportion. In contrast

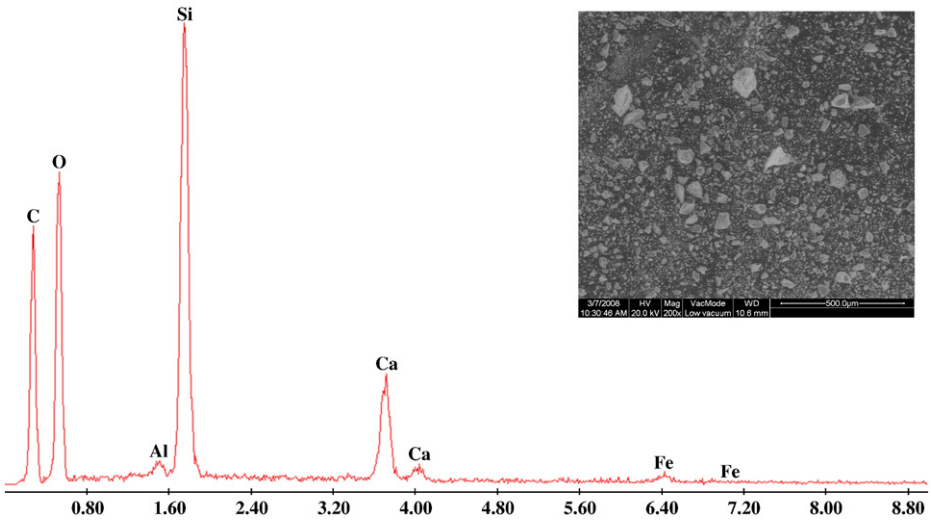

Fig. 13. SEM recording of a prepared aggregate powder (corner) and EDX.

with the groups defined with XRD, the red aggregate belongs to this second group, because it has a comparable amount of Si and only a small amount of calcium (Ca). Group 3 has a smaller mutual percentage of Si, while the mutual percentage of Ca is higher. And finally, group 4 is determined by the occurrence of magnesium (Mg).

The powders are heated with an electric oven to different target temperatures, which are held constant for approximately 2 h. The temperature rate of the furnace is around 30 °C/min and the target temperature is raised every 50 °C, resulting in the following temperatures: 120 °C, 200 °C, 250 °C, …, 1100 °C and 1150 °C. The colour of the heated powders is measured between successive heating regimes with an X-rite SP60 spectrophotometer according to the CIE Lab-colour space. In this colour system 'L' is the lightness with values between 0 (black) and 100 (white), while 'a' is spread between magenta (positive values) and green (negative values) and 'b' is positioned between yellow (positive values) and blue (negative values). Plotted in a chart, with the 'a' on the *X*-axis and the 'b' on the *Y*-axis, orange is situated in the right top corner, faded over red to purple in the right bottom corner. In the left top corner, green is found fading to blue in the left bottom corner and along the bottom of the gamut. Between green and orange, yellow is spread. Grey colours, typically for concrete, are located more in the centre of the 'ab'-chart and further spread around the *Z*-axis, which is the 'L' parameter. Fig. 14 depicts the colour change of the investigated aggregates spread in the 'ab'-chart. Each aggregate group as defined above has its own typical colour path. The form of the path of groups 1 and 2 is nevertheless similar: an increase of both the 'a' and the 'b' values from 20 °C to approximately 700 °C, which tends towards a more orange tint. From there, a decrease of the 'a' and 'b' values is noticeable, this is towards a more grey tint. Above 1000 °C, the colour turns gradually more to white, except for the aggregate 'white–yellow' which alters further to a grey–purple tint. Around 250 °C and 950 °C, the colour changes with a greater amount. The colour paths of the aggregates of group 2 lie close to each other. On the other hand, for group 1 the aggregate 'white–yellow' turns further towards an orange tint at 700 °C than the aggregate 'white', which could be attributed to the occurrence of a certain amount of iron in the aggregate 'white–yellow'. When this aggregate is heated to 250 °C, the yellow part will change into a pink tint which is perceptible when heating an ungrounded grain. For group 3, the 'a' parameter jumps to a higher value around 250 °C, from where it increases slowly to a maximum around 450 °C. A decreasing branch is visible till approximately 700 °C, from where the 'a' value remains more or less constant. However, at 950 °C the 'a' value of the aggregate 'blue' decreases. For the 'b' value, a small increase occurs from the original value to around 450 °C, from where the 'b' value of the aggregate 'brown' keeps dropping till around 950 °C, from where it further increases till 1150 °C. On the other hand, the aggregate 'blue' decreases only to 700 °C, from where it continues to increase to a maximum around 950 °C. Beyond 950 °C, the 'b' value of the aggregate 'blue' drops till around 1050 °C, from where it further increases till 1150 °C. At 1100 °C, the aggregate 'blue' has travelled to a white colour with yellow tint, while the aggregate 'brown' has turned into orange. Group 4, this is the aggregate 'green', keeps its original colour till around 200 °C, from where both the 'a' and 'b' values keep increasing to a maximum around 950 °C. Above 950 °C, the path takes a loop and goes back on its way. This aggregate 'green' shows a remarkable colour shift from pale green to orange. During the colour alterations, the L parameter of the aggregates 'brown' and 'green' drops around 250 °C from a value of 70 to 60, respectively 75 to 60. Beyond 1000 °C the L parameter of the aggregate 'brown' increases back to its original value at 1150 °C. While for the aggregate 'blue' the value of L increases at 600 °C from around 73 to 88. The other aggregates have a more or less constant value of L between 75 and 85.

All aggregates show an alteration to a more reddish tint when heated to 250 °C, which is supposed to be caused by the oxidation of

Table 4
EDX results.

At %	Group 1		Group 2			Group 3		Group 4
	White	White–yellow	Yellow–brown	Brown–iron	Red	Brown	Blue	Green
MgK	–	–	–	–	–	–	–	2.55
AlK	1.29	–	3.73	7.12	1.92	2.24	–	4.92
SiK	97.30	96.76	90.43	86.93	89.94	72.40	56.28	85.03
KK	–	–	3.74	4.01	1.09	–	–	–
CaK	1.42	–	–	–	3.60	22.17	43.73	–
FeK	–	3.24	2.12	1.95	3.47	3.21	–	7.51

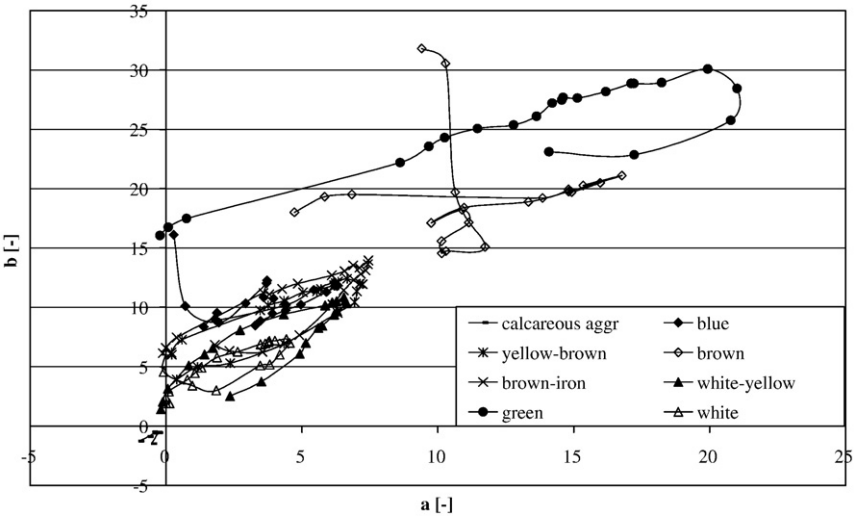

Fig. 14. Colour development with temperature of the aggregates.

the iron in the aggregates. This assumption seems to be right, since the aggregates with the greatest amount of iron (green, brown) do show a larger colour shift. However, also for the aggregates where no iron could be detected (white, blue), a shift is recognisable.

The colour path of calcareous aggregates is also studied with the spectrophotometer and plotted in Fig. 14. The colour is measured for the temperature region 20 °C to 600 °C, directly on the sawn aggregates surface, without grinding. No large displacements appear in the 'ab'-graph when compared to the colour alterations of the siliceous aggregates: the colour transforms from black to all kinds of blue. However, visible observation shows at 700 °C a colour shift to white due to decarbonation.

The observed colour alterations can be used to determine the temperature history inside a concrete element. A drilled core can be sliced into discs parallel to the exposed surface, from which the aggregates can be used for further study with colorimetry and EDX. This paper covers 3 distinct colour paths for heated siliceous aggregates and describes test values for 7 types of aggregates. Comparison of the measured colours from the drilled core with the test values should provide enough information to quantify the temperatures reached inside the concrete.

5. Conclusions

To assess the residual strength of a concrete structure, information about the temperatures reached in the concrete is needed. These temperatures can be determined in different ways on the basis of cores drilled out of the structure. Once these temperatures are estimated, the concrete strength and thus the overall damage of the members can be assessed based on known relationships between strength loss and temperature.

A first method to reveal the temperature history of a heated concrete structure is by studying the samples with a scanning electron microscope (SEM). This technique provides a determination of the depth at which the cement paste has lost ettringite (>70 °C) and portlandite (>450 °C). The observed increase in porosity of the cement stone and cracking around the fine and coarse aggregates also indicate heating.

A second method is based on the use of polarising and fluorescent microscopy (PFM). According to which light setting is used, different physico-chemical transformations can be observed. Under plain polarised transmitted light (PPTL) the breakdown of ettringite in the pores (>70 °C), the oxidation of the iron oxide in the aggregates (about 300 °C), as well as the development of cracks can be studied. Under UV fluorescent light (UVFL), the change in fluorescence due to the loss of the free water (>105 °C), and the dissociation of the sand particles in some siliceous aggregates (about 300 °C) can be observed. Under cross polarised light (CPL) the dissociation of portlandite (400–600 °C) is visible.

A third method, studied in this paper, is the colour alteration of the aggregates used in concrete. From a batch of siliceous aggregates, the most representative colours are selected and classified in 4 groups on the basis of their mineralogical (XRD) and chemical (EDX) composition. Three main different colour paths are found. The main trend is a discoloration towards orange, probably due to the oxidation of the present iron. The most notable shifts are at 250 °C (oxidation of the iron), 700 °C and 950 °C. A drilled core can be sliced in different discs parallel to the exposed surface. From these discs, the aggregates can be obtained and studied for colour and composition. Matching these results on the colour path graph for each depth should allow the assessment of the temperature distribution in the concrete. Also, the colour change of calcareous aggregates has been studied, where the colour alters from black to blue for temperatures up to 600 °C. These changes are small compared to the colour shifts of siliceous aggregates. However, at 700 °C, the colour turns into white due to decarbonation.

Acknowledgements

The thin sections were manufactured by TNO Built Environment and Geosciences in Delft and analysed in cooperation with Dr. J. A. Larbi and Dr. T. G. Nijland of TNO. The ESEM images were taken at Microlab of TU Delft under the supervision of Professor M. R. De Rooij. The authors would like to thank these persons for providing their expertise and services to explore by polarising fluorescent microscopy and ESEM the microstructural changes of ordinary Portland cement concrete exposed to fire.

References

[1] A.K. Tovey, E. Mellor, R.H. Jackson, C.D. Jones, J.C.M. Forrest, Technical Report No. 33 — Assessment and Repair of Fire-damaged Concrete Structures, Concrete Society, Camberly, 1990.
[2] L. Taerwe, E. Annerel, Loading test on a retrofitted pretensioned concrete girder after fire, in: M.G. Alexander, H.-D. Beushausen, F. Dehn, P. Moyo (Eds.), Concrete Repair, Rehabilitation and Retrofitting II, Proceedings of ICCRRR 2008, Taylor & Francis Group, London, 2009, pp. 1061–1067.
[3] EN 1992-1-2: 2004, Eurocode 2: Design of Concrete Structures — Part 1–2: General Rules — Structural Fire Design, CEN, Brussels, 2004.
[4] E. Annerel, L. Taerwe, Approaches for the assessment of the residual strength of concrete exposed to fire, in: J.P.C. Rodrigues, G.A. Khoury, N.P. Høj (Eds.), Proceedings of the International Workshop: Fire Design of Concrete Structures,

from Materials Modelling to Structural Performance, University of Coimbra, Coimbra, 2007, pp. 489–500.
[5] X. Liu, Microstructural Investigation of Self-compacting Concrete and High-performance Concrete during Hydration and after Exposure to High Temperatures, PhD thesis, Ghent University, Ghent, 2006.
[6] J. Larbi, T.G. Nijland, Unraveling the temperature distribution in fire-damaged concrete by means of PFM microscopy: outline of the approach and review of potentially useful reactions, Heron 46 (4) (2001) 253–264.
[7] R. Felicetti, Digital camera colorimetry for the assessment of fire-damaged concrete, in: P.G. Gambarova, R. Felicetti, A. Meda, P. Riva, Proceedings of the Workshop: Fire Design of Concrete Structures: What now? What next? fib Task Group 4.3 'Fire Design of Concrete Structures', Milan, 2004, pp. 211–220.
[8] G. Ye, Experimental Study and Numerical Simulation of the Development of the Microstructure and Permeability of Cementitious Materials, PhD thesis, TU Delft, Delft, 2003.
[9] G.A. Khoury, Y. Anderberg, K. Both, J. Fellinger, N.P. Høj, C. Majorana, Fib Bulletin 38: Fire Design of Concrete Structures — Materials, Structures and Modelling, State-of-the art Report, International Federation for Structural Concrete (fib TG 4.3.1), Lausanne, 2007.
[10] L. Taerwe, P. Bamonte, K. Both, J.-F. Denoël, U. Diederichs, J.-C. Dotreppe, R. Felicetti, J. Fellinger, J.-M. Franssen, P.G. Gambarova, N.P. Høj, T. Lennon, A. Meda, Y. Msaad, J. Ožbolt, G. Periškić, P. Riva, F. Robert, A. Van Acker, Fib Bulletin 46: Fire Design of Concrete Structures — Structural Behaviour and Assessment, State-of-the art Report, International Federation for Structural Concrete (fib TG 4.3.2), Lausanne, 2008.
[11] J. Elsen, N. Lens, T. Aarre, D. Quenard, V. Smolej, Determination of the w/c ratio of hardened cement paste and concrete samples on thin sections using automated image analysis techniques, Cement and Concrete Research 25 (1995) 827–834.
[12] U.H. Jakobsen, D.R. Brown, Reproducibility of w/c ratio determination from fluorescent impregnated thin sections, Cement and Concrete Research 36 (2006) 1567–1573.
[13] L. Alarcon-Ruiz, G. Platret, E. Massieu, A. Ehrlacher, The use of thermal analysis in assessing the effect of temperature on a cement paste, Cement and Concrete Research 35 (2005) 609–613.